

STUDY OF HYPERFINE PARAMETERS IN Co-DOPED TIN DIOXIDE USING PAC SPECTROSCOPY

Juliana M. Ramos¹, Artur W. Carbonari¹, Thiago Martucci¹, Messias S. Costa¹, Rajendra N. Saxena¹, R. Vianden², P. Kessler², T. Geruschke² and M. Steffens²

¹ Instituto de Pesquisas Energéticas e Nucleares (IPEN / CNEN - SP)
Av. Professor Lineu Prestes, 2242
05508-000 São Paulo, SP
emrjmr@superig.com.br

² Helmholtz - Institut für Strahlen- und Kernphysik (HISKP- Bonn)
Rheinische Friedrich-Wilhelms-Universität Bonn
Nussallee 14-16
D-53115 Bonn, Germany
vianden@hiskp.uni-bonn.de

ABSTRACT

PAC technique has been used to measure the hyperfine interactions in nano-structured powder samples of semiconducting SnO₂ doped with Co. The aim of this work is to compare the results of PAC measurements using two different techniques of introducing the radioactive ¹¹¹In probe nuclei in the sample of SnO₂ doped with Co. The perturbed gamma-gamma angular correlation (PAC) spectroscopy is used for the measurements of the magnetic hyperfine field (MHF) and the electric field gradient (EFG) at ¹¹¹Cd sites in SnO₂ doped with 1% and 2% Co. The measurement of EFG is used to study the defects introduced in the semiconductor material and also for the identification of different phases formed within the compound. The techniques utilized for introducing the radioactive ¹¹¹In in the sample are the ion-implantation using radioactive ion beam of ¹¹¹In and the chemical process in which ¹¹¹InCl₃ solution is added during the preparation of SnO₂ doped with Co using sol gel method [1]. The ion-implantation of ¹¹¹In in SnO₂ doped with Co was carried out using the University of Bonn ion-implanter with beam energy of 160 keV. The PAC measurements were carried out with four BaF₂ detector gamma spectrometer in the temperature range of 10-295 K. The results show no significant difference in the values of hyperfine parameters. Both techniques show practically the same electric quadrupole interaction for the substitutional site. The results were compared with previous PAC and Mössbauer measurements of SnO₂ powder samples using ¹¹¹In-¹¹¹Cd probe [1,2].

1. INTRODUCTION

Tin dioxide is a n-type semiconductor [1] with important properties like chemical stability, optical transparency in the visible region and band gap of 3.6 eV [3]. There are also many technological applications like gas sensor [4], varistors [5], solar cells [6]. This oxide is an excellent candidate for diluted magnetic semiconductors (DMS) when is doped with cobalt [7]. The DMS form a new class of semiconductor materials that have been intensively studied in recent years due to enormous technological potential.

The new emerging field of electron spin transfer in semiconductors (spintronics) is to use degrees of freedom, the charge and the spin of electrons in semiconductors. The use of spin in addition to the charge has a huge potential to increase data processing and the ability to store them from the current devices, besides being very promising for a new class of devices such as polarized light emitting diodes, chips that integrate the functions of processing and memory and transistors of ultra-low power [8,9]. A key condition to make these spin-based

devices is that the matrix material present ferromagnetic ordering temperature (TC) above room temperature. In addition, one must have both, the injection of spin polarized carriers and their electrical transport.

The search for magnetic semiconductors is not new, the first observation of ferromagnetism in semiconductors was reported in the sixties, with the observation of ferromagnetism in EuX (X = O, S, Se) [10] with $T_C = 69$ K. After the discovery of room temperature ferromagnetism in TiO₂ doped with 2% Co by Matsumoto et al [11] much attention was devoted to wide band-gap semiconductor oxides doped with transition metals. The occurrence of ferromagnetism at room temperature has been reported in some oxides doped with transition metals: TiO₂, ZnO, CuO, SnO₂ e In₂O₃ [12] and gradually it became clear that the ferromagnetism in lightly doped oxide semiconductor (DMOS) is a widespread phenomenon in various materials. More details on the development of semiconductors doped oxides can be found in review articles written by Coey [12]. Review articles on materials and spintronics DMS can be found in references 13, 14 e 15.

Fitzgerald et al [7] reported using Mössbauer Spectroscopy that the Co-doped (5%) bulk samples were paramagnetic at room temperature. Misra et al [3] studied powder samples doped with different concentrations of Cobalt using Electron paramagnetic resonance, and reported that Co doping ($\leq 1\%$) produces ferromagnetism at room temperature most probably due to oxygen vacancies and/or changes in carrier concentration. Their work also reported that at higher Cobalt concentrations ($\sim 12\%$), no ferromagnetism was observed. In our previous work [1], using PAC spectroscopy, we observed no ferromagnetism behavior for Co-doped powder samples with concentrations in the range of (2-5%).

Shek et al [16] studied the effect of oxygen deficiency on Raman Spectra of nano-SnO₂ specimens, observing that high temperature annealing achieves the ideal stoichiometry of nano-SnO₂. Due to this fact, in this work we used low and high annealing temperature to investigate the influence of the oxygen vacancies or defects in the hyperfine parameters. In tin dioxide doped with elements of valence +2 an increase in the concentration of extrinsic defects is observed. Oxygen vacancies cause an increase in the diffusion coefficient of ions [17]. We can find several articles reporting ferromagnetism at room temperature in Co-doped SnO₂ thin films. K Gopinadhan et al [18] observed at room temperature ferromagnetic moment in thin films doped with 10% of Co produced by spray pyrolysis. They also observed that the film with 15% of Co showed a weaker ferromagnetic behavior due to the formation of the secondary phase (Co₃O₄). Ogale et al [19] reported ferromagnetism for the films doped with 5% of Co with a giant magnetic moment of $7.5 \pm 0.5 \mu_B/\text{Co}$ with Curie temperature close to 650 K. Nguyen Hoa Hong et al [20] also observed a giant magnetic moment for thin films doped with 5% of Cr.

1.2. PAC Technique

PAC measurements provide information about hyperfine interactions between extranuclear electromagnetic fields and nuclear moments of a radioactive probe nucleus placed on a particular atomic site of the crystal. Where as the energy separation of the nuclear sublevels

is directly measured by the resonance process in the experiments of Mössbauer spectroscopy and nuclear magnetic resonance, the precession frequency is measured in the PAC experiment. The precession frequency is determined from the observed modulations of perturbed gamma-gamma angular correlation spectra and provides information about electric and magnetic fields generated by electronic and ionic neighborhood of the probe nuclei.

PAC technique measures the time dependence of the γ -ray emission pattern. This evolution in time is caused by hyperfine interactions. The angular distribution of the emission pattern is given by the correlation function (1):

$$W(q,t) = 1 + A_{22}G_{22}(t)P_2 \cos(\theta) \quad (1)$$

Hyperfine interactions cause a precession of the emission pattern described by the dependent perturbation factor $G_{22}(t)$. Experimental measurement of $G_{22}(t)$ permits the determination of magnetic (2) and quadrupole frequencies (3):

$$\omega_L = \frac{g\mu_N B}{\hbar} \quad (2)$$

$$\omega_Q = \frac{eQV_{zz}}{4I(2I-1)\hbar} \quad (3),$$

from which the hyperfine magnetic field B and the largest component (V_{zz}) of the EFG can be deduced.

2. EXPERIMENTAL

2.1. Ion-implantation

The samples were prepared using the sol gel method, a methodology established to produce nanoparticles. More details about this methodology can be found in the reference [1]. Pellets of 200mg were made under a pressure of 5 T/cm² and were subject to a thermal treatment of 14 hours in flowing nitrogen as shown in the fig. 1.

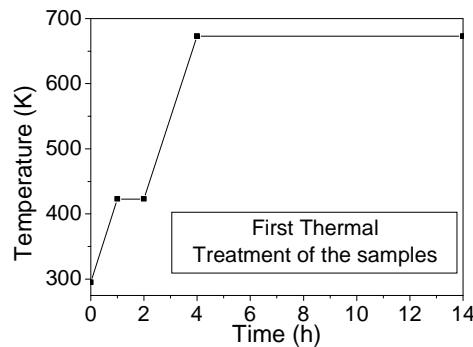


Figure 1.: Thermal treatment of the samples (pellets and powder) were done from room temperature to 423K during 1h, maintaining at this temperature for 1h, then increasing to 673K during 2h, and maintaining at this temperature for 10h.

The ^{111}In activity was ion implanted using the University of Bonn ion implantation machine, with fluence of roughly 10^{12} ions/cm² and energy of 160keV. A rapid thermal annealing (RTA) was carried out after the ion implantation, at a temperature of 723K for 10 minutes (for the sample doped with 1%Co) and 653K for 10 minutes (for the sample doped with 2%Co). The pellets were measured at 295K in PAC spectrometer with 4 detectors in the University of Bonn.

2.2. Addition of $^{111}\text{InCl}_3$ solution

An additional set of samples were prepared using sol-gel method and measured in the powder form. Approximately 30 μCi of $^{111}\text{InCl}_3$ solution was added to the solution of tin and cobalt dissolved in acid before the formation of gel. The thermal treatment given to the samples was same as in the previous cases. The powders were measured at 295K in PAC spectrometer at IPEN in São Paulo with a four BaF₂ detector spectrometer.

3. RESULTS AND DISCUSSION

3.1. Characterization of samples

All the samples were examined by X-Ray diffraction (XRD) using Cu K α radiation and scanning electron microscopy (SEM). Using Scherer's equation [21] the average particle sizes of 16 nm were deduced for the pellet doped with 2% of Co after the first thermal treatment. Within the resolution of XRD measurements, no impurity phases were identified as shown in Fig. 2. The results showed only a single phase with $P4_2/mnm$ space group corresponding to the rutile-type structure after the annealing at 653K in the muffle furnace.

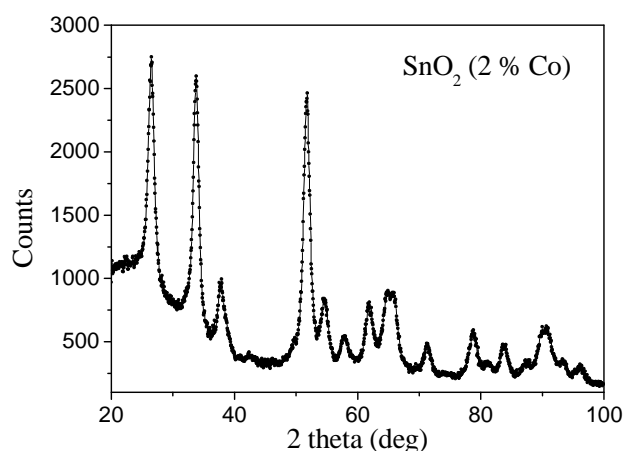


Figure 2. X-ray diffractogram of the tin dioxide pellet doped with 2% of Co.

The nanoparticles sizes of the sample doped with 2% of Co were also determined by scanning electron microscopy (SEM) and the results indicate that there is no significant difference in the nanoparticles sizes after the first (553K) and the second (653K) thermal treatment. Fig.3 shows a SEM image for pure SnO₂ (a) and doped with 2% of Co (b). These samples prepared with the same annealing temperature of 653K. The EDS image (Fig. 4) Indicates that only Sn, O and Co are present in the sample. These were the samples measured at Bonn University.

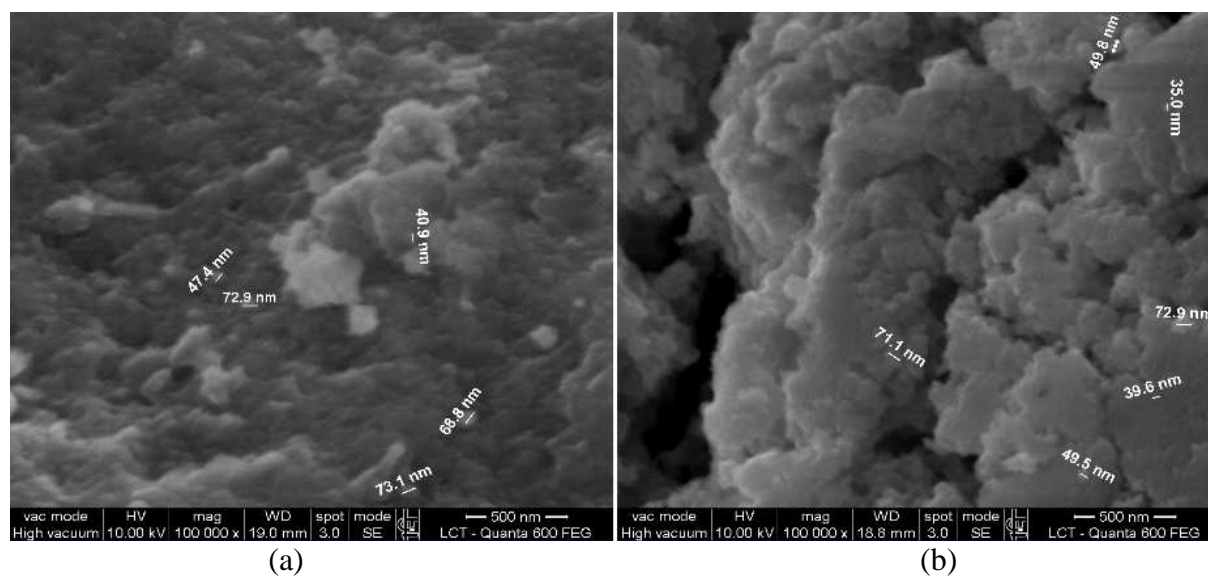


Figure 3. SEM Photograph of SnO₂ sample doped 2% of Co annealed at 553 K (a) and 673 K (b)

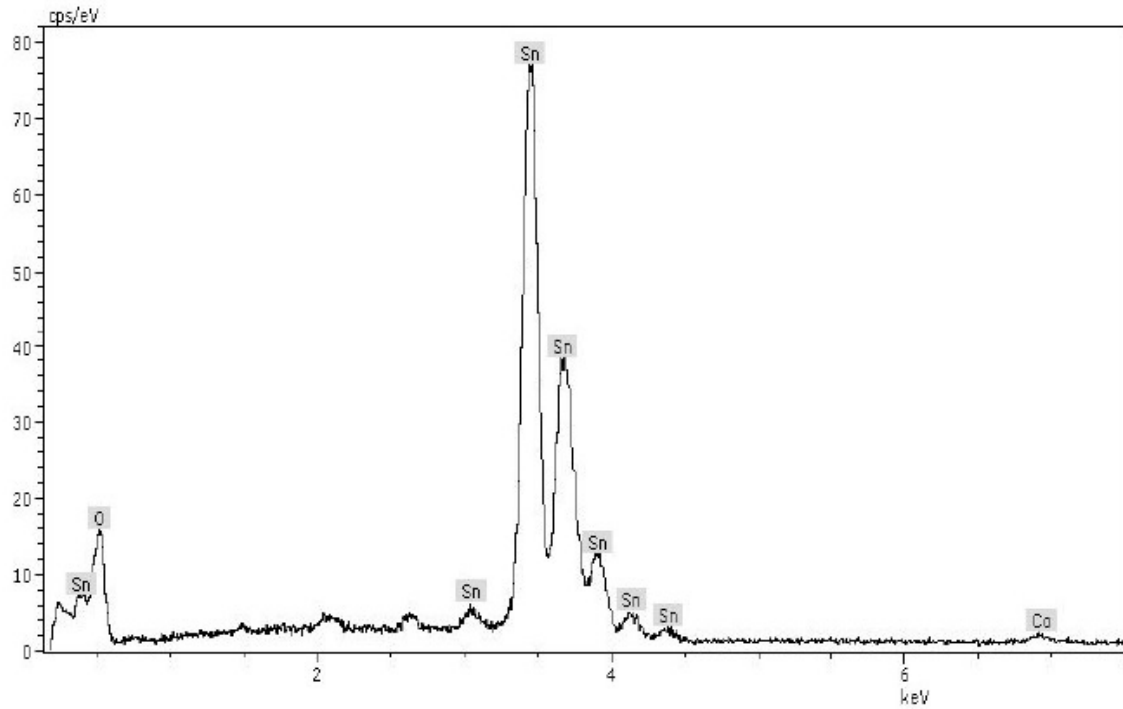


Figure 4: EDS image of pellet showing Sn, O and Co

3.2. PAC results

The PAC spectra of the tin dioxide pellets doped with 2% of Co measured at Bonn University are shown in fig. 5. All the samples were measured at 295 K. The fitted hyperfine parameters of the spectra are given in table 1.

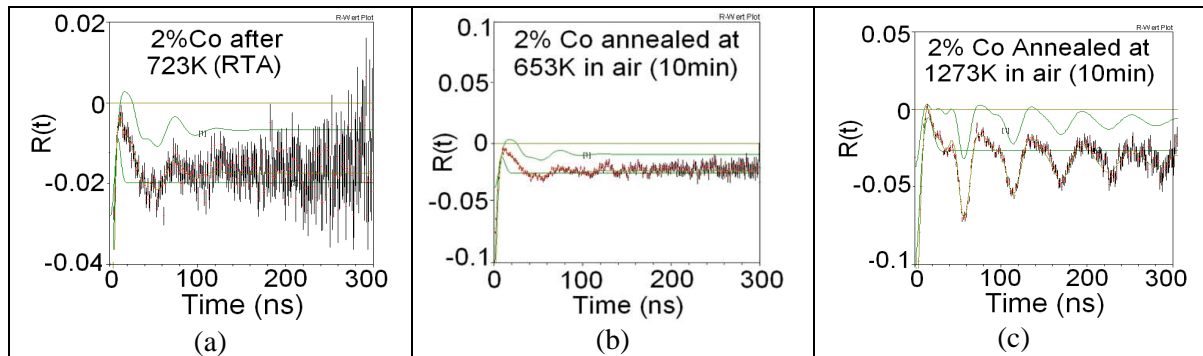


Figure 5: PAC spectra of the SnO₂ doped with 2% Co annealed at different temperatures

Table 1. Hyperfine Parameters of the ¹¹¹In-implanted SnO₂ pellets doped with 2% of Co

	Site 1 (substitutional)				Site 2			
Spectrum	ν_Q (MHz)	η	fraction (%)	δ (%)	ν_Q (MHz)	η	fraction (%)	δ (%)

(a)	104	0.5	27	16	166	0.8	73	61
(b)	102	0.5	27	18	160	0.8	73	61
(c)	110	0.2	42	16	94	1.0	58	51

The PAC spectra of the tin dioxide pellets doped with 1% of Co measured at Bonn University are shown in fig. 6. The fitted hyperfine parameters of the spectra (d) and (e) are given in table 2.

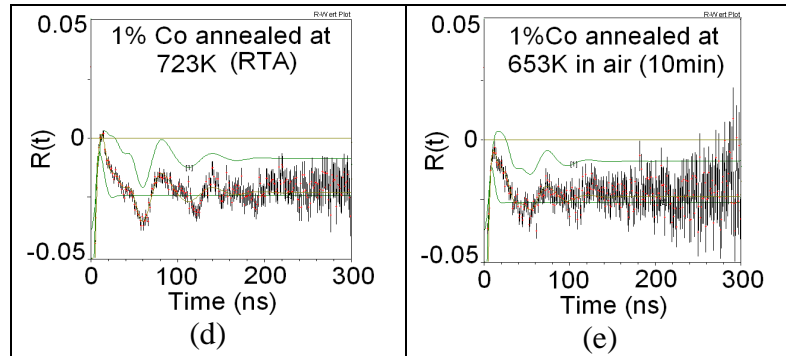
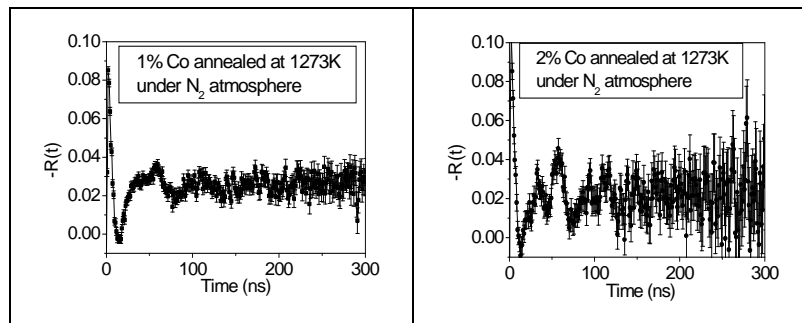


Figure 6. PAC spectra of SnO₂ doped with 1% of Co annealed at 723 K and 653 K

Table 2. Hyperfine Parameters of the ¹¹¹In-implanted SnO₂ pellets doped with 1% of Co

Spectrum	Site 1 (substitutional)				Site 2			
	ν_Q (MHz)	η	fraction (%)	δ (%)	ν_Q (MHz)	η	fraction (%)	δ (%)
(d)	109	0.3	0.3	27	197	0.5	73	47
(e)	104	0.5	0.5	27	173	0.7	73	59

The PAC spectra of the powder samples doped with 1% and 2% of Co measured at IPEN are given in fig. 7. The samples were annealed in nitrogen atmosphere at 1273 K for 10 hours. The fitted hyperfine parameters of the spectra are given in table 3.



(f)	(g)
-----	-----

Figure 7. PAC spectra of SnO₂ powder samples measured at IPEN.

Table 3. Hyperfine Parameters of SnO₂ powder samples doped with 1% of Co (f) and doped with 2% of Co (g).

Spectrum	Site 1 (substitutional)				Site 2			
	ν_Q (MHz)	η	fraction (%)	δ (%)	ν_Q (MHz)	η	fraction (%)	δ (%)
(f)	116	1.0	40	17	127	0	60	19
(g)	116	0.3	22	5	126	0.7	78	53

Bibiloni et al [2] studied pure SnO₂ powders samples using PAC spectroscopy. Their results show only electric quadrupole interactions. They observed an electric quadrupole frequency (ν_Q) of 91MHz for the substitutional site (measured at 300K). Their samples were oxidized in air at 483K for 20 hours and reoxidized in air at 1103K for 2 hours. Our SnO₂ pellet doped with 2% of Co annealed at 1273K in air for 10 min (spectra c) was measured at Bonn and present $\nu_Q= 94$ MHz. The same pellet present for the other site $\nu_Q= 110$ MHz and can be compared with the same Bibiloni sample measured at 523K which present $\nu_Q= 112$ MHz. The powder samples measured at IPEN could also be compared with the same Bibiloni sample. Our powder samples (doped with 1 or 2% of Co – spectrum f and g) present for the substitutional site $\nu_Q= 116$ MHz and the Bibiloni sample present $\nu_Q= 117$ MHz when is measured at 1073K. These comparisons revealed that for the substitutional site, the element Co did not influence the electric quadrupole frequency. Our other values for the substitutional site of the both kind of samples (powder or ion-implanted pellet) are in the range of 102-109 MHz which are very closed to the compared results.

The electric quadrupole frequency of the powder samples doped with 1% and 2% of Co (spectrum f and g) are similar for both sites. Only the asymmetry parameter is different, what means that the symmetry depends on the cobalt percentage in the sample.

Our non substitutional site of the pellet doped with 2% of Co presents after annealing at 653K and 723K, respectively, $\nu_Q= 160$ MHz and 166MHz. These values are closed to Bibiloni's results [2] to the sample measured at 150K which presents 197MHz. Our non substitutional site of the pellet doped with 1% of Co presents after annealing at 723K $\nu_Q= 197$ MHz and Bibiloni's sample measured at 17K and 300K presents, respectively, 197MHz and 198MHz. The asymmetry parameter values of the substitutional site of our samples decreases with increasing annealing temperature. For the other site, the asymmetry parameter increases with increasing annealing temperature and the asymmetry parameter of the Bibiloni et al [2] samples also increases with increasing the measurement temperature (from 0.33 to 0.6). Only the asymmetry parameter of the powder sample doped with 1% of Co (spectra f) is not in accordance.

The pellets doped with 2% of Co presents an increasing in the fraction of the substitutional site when increasing annealing temperature. The same behavior is observed in the Bibiloni et al [2] samples: the fraction of the substitutional site is increasing with increasing measurement temperature. During the measurement of Bibiloni occurred the thermal expansion of the crystalline lattice and the same phenomenon occurs with our samples during the annealing process, revealed in the SEM photograph results.

One charge state of tin is Sn^{4+} . The Co could have two possible charge states Co^{2+} ($3d^7$) and Co^{3+} ($3d^6$). In the case of the Co^{3+} the valence is different of the Sn^{4+} , what could influence the production of defects. When two atoms of Sn^{4+} are replaced by two atoms of Co^{3+} more oxygen vacancies would be introduced in the sample [22]. The role of the defects in tin dioxide is not new because of the variety of technological applications of this semiconductor. Discussion about defect chemistry of SnO_2 may play an important role for the ferromagnetic properties. J. M. Coey et al [23] analyzed the ferromagnetism origin in terms of a model of indirect exchange via shallow donors, considering thin films. Bulk samples do not have a lot of defects as in thin films, and defects are difficult to control in sample preparation. Our samples did not show ferromagnetism through the hyperfine parameters even with the presence of defects. The site of the defects presents a fraction bigger than the substitutional fraction. The same behavior is observed and discussed in the Bibiloni et al. work [2].

4. CONCLUSION

The results for the sample doped with 1% of Co are quite similar to the results of the samples doped with 2% of Co. We can also compare the hyperfine parameters with our previous work [1] for the samples doped with 2% of Co. In this work it was observed electric quadrupole interactions characterized by two different frequencies. One of them with $\nu_Q \sim 102\text{-}115$ MHz, $\eta \sim 0.1\text{-}0.5$, and $\delta \sim 12\text{-}18\%$, which changes very little with temperature and has been assigned to ^{111}Cd at Sn sites in SnO_2 structure. The results are in agreement with [1] that presents $\nu_Q \sim 115$ MHz, $\eta \sim 0.1$, and $\delta \sim 12\%$ and with the reference [2]. The second one is characterized by a wider distributed frequency that changes with temperature with values in the range of $94\text{-}197$ MHz and asymmetry parameter varying from 0.4 to 1 and assuming the biggest fraction. This interaction was associated with ^{111}Cd probes trapped in defects near the surface of the nanoparticles. The results are in agreement with [1] that presents values of ν_Q in the range of $120\text{-}180$ MHz and asymmetry parameter varying from 0.4 to 1.

The results shows no significant changes in the values of hyperfine parameters of the tin site in the crystall lattice. Both techniques reveals the same behaviour of the EFG for the samples. After all we can conclude that it was observed the presence of only pure electric quadrupole interaction. Both techniques reveal the same electric quadrupole interaction for the substitutional site.

ACKNOWLEDGMENTS

A.W.C. and R.N.S. thankfully acknowledge the support provided by CNPq in the form of research fellowships. J.M.R. also thanks the support provided by CNEN and CNPq

in the form of scholarships. Partial financial support for this research was provided by the Fundação de Amparo a Pesquisa do Estado de São Paulo (FAPESP).

REFERENCES

- [1] Ramos J. M. et al, "Electric quadrupole interactions in nano-structured SnO₂ measured with PAC spectroscopy," *Hyperfine Interactions*, **197** pp.239-244 (2010).
- [2] A. G. Bibiloni et al. "Hyperfine interaction between indium atoms and oxygen vacancies in stannic oxide," *Physical Review B*, **38** 20-25 (1988).
- [3] Sushil K. Misra et al. "Magnetic resonance studies of Co²⁺ ions in nanoparticles of SnO₂ processed at different temperatures," *Journal of Applied Physics*, **99** pp.08M106/1-08M106/3 (2006)
- [4] T. Sequinel et al, "Sinterização e caracterização de segunda fase em sistemas SnO₂-ZnO," *Cerâmica*, **51** pp.269-273 (2005).
- [5] M. M. Oliveira et al, "Desenvolvimento de varistores à base de SnO₂ para aplicação em redes de alta tensão," *Cerâmica*, **52** pp.149-154 (2006).
- [6] Nam-Gyu Park et, "Photovoltaic characteristics of dye-sensitized surface-modified nanocrystalline SnO₂ solar cells," *Journal of Photochemical and Photobiology A: Chemistry*, **161** pp.105-110 (2004).
- [7] C. B. Fitzgerald et al, "SnO₂ doped with Mn, Fe or Co: Room temperature dilute magnetic semiconductors," *Journal of Applied Physics*, **95** pp.7390-7393 (2004).
- [8] S. von Molnar S and D. Read, "New materials for semiconductor spin-electronics," *Proceedings of the IEEE*, **91** pp. 715-726 (2003).
- [9] S. A. Wolf et. al, "Spintronics: A Spin-Based Electronics Vision for the Future," *Science*, **294** pp.1488-1495 (2001).
- [10] B. T. Matthias, R. M. Bozorth, and J. H. Van Vleck, "Ferromagnetism in Solid Solutions of Scandium and Indium," *Physical Review Letters*, **7** pp.7-9 (1961).
- [11] Y. Matsumoto, M. Murakami, T. Shono, T. Hasegawa *et al.*, "Room-Temperature Ferromagnetism in Transparent Transition Metal-Doped Titanium Dioxide," *Science*, **292** pp.854-856 (2001).
- [12] J. M. D. Coey, "Dilute Magnetic Oxides," *Current Opinion in Solid State and Materials Science*, **10** pp. 83-92(2006).
- [13] S. J. Pearton et al, "Wide band gap ferromagnetic semiconductors and oxides," *Journal of Applied Physics*, **93** pp.1- 13(2003).
- [14] S. J. Pearton et. al, "Advances in wide bandgap materials for semiconductor spintronics," *Materials Science and Engineering R*, **40** pp.137-168 (2003).
- [15] A. H. MacDonald, P. Schiffer, and N. Samarth, "Ferromagnetic semiconductors: moving beyond (Ga,Mn)As," *Nature Materials*, **4** pp.195-202 (2005).
- [16] C. H. Shek, G. M. Lin and J. K. L. Lai, "Effect of oxygen deficiency on the Raman spectra and hyperfine interactions of nanometer SnO₂," *Nanostructured Materials*, **11** pp.831-835 (1999)
- [17] Magalhães, E. C. S, *Propriedades Ópticas de Filmes Finos de Dióxido de Estanho Puro e Dopado com Flúor*, Bahia, Brasil, (2006).

- [18] K. Gopinadhan et al, "Cobalt-substituted SnO₂ thin films: A transparent ferromagnetic semiconductor," *Journal of Applied Physics*, **99** pp.126106-126109 (2006).
- [19] S. B. Ogale et al, "High Temperature Ferromagnetism with a Giant Magnetic Moment in Transparent Co-doped SnO_{2-δ}," *Physical Review Letters* **91** pp.077205/1-077205/4 (2003).
- [20] Nguyen Hoa Hong et al, "Transparent Cr-doped SnO₂ thin films: ferromagnetism beyond room temperature with a giant magnetic moment," **17** pp.1697-1702 (2005).
- [21] A. L. Patterson, "The Scherrer Formula for X-Ray Particle Size Determination," *Physical Review*, **56** pp. 978-982 (1939).
- [22] C. B. Fitzgerald et al, "Magnetism in Diluted Magnetic Oxide Thin Films Based on SnO₂," *Physical Review B*, **74** pp.115307/1-115307/10 (2006).
- [23] J.M. Coey, M. Venkatesan and C.B. Fitzgerald, "Donor impurity band exchange in dilute ferromagnetic oxides," *Nature Materials*, **4** pp.173-179 (2005).